Transition Mechanisms and Phases of Hexane Physisorbed on Graphite

C.L. Pint[*,†], M.W. Roth[*] and C. Wexler[**]

[*]University of Northern Iowa, Cedar Falls, IA, 50614
[**]University of Missouri-Columbia, Columbia, MO, 65211
[†]Electronic mail: cpint@uni.edu

ABSTRACT

We present the results of molecular dynamics (MD) simulations of hexane adsorbed onto graphite at submonolayer ($\rho<1$), monolayer ($\rho=1$), and supermonolayer ($\rho>1$) coverages. We find the presence of three phases, the low temperature solid herringbone (HB) phase, the intermediate-nematic (IN) phase, and the isotropic fluid phase. For submonolayer coverages, we find that the IN phase disappears except for coverages very close to completion, however, for $\rho>1$ we find an augmented IN phase with most molecules rolled normal to the substrate. We also observe for $\rho<1$ the presence of fluid-filled domain walls when taking the tetrahedral symmetry of the endgroups into account. Through variations we study the formation of gauche molecules and conclude that both phase transitions observed exhibit much out-of-plane tilting, with only a *small* presence of conformation changes near the melting transition. We conclude that in-plane space plays an important role in the phases and transitions in this system.

Keywords: molecular dynamics, adsorption, *n*-alkanes, hexane, graphite

1 INTRODUCTION

Hexane, (C_6H_{14}) is a member of the family of straight-chained *n*-alkanes whose members differ mainly in their length and whose study is appealing due to the vast industrial applications (e.g. adhesion, lubrication, wetting, etc.) that these molecules exhibit as adsorbates. Hexane is a short-chained even numbered *n*-alkane whose properties are general to a subset of similar even *n*-alkanes [1] with $6<n<10$ in that the phases exhibited by each involve an isomorphic herringbone (HB) phase at low temperatures, followed by a transition into an intermediate phase, where experiment observes a solid and liquid in coexistance.

Experimentally, the behavior of monolayer and submonolayer hexane on graphite is well studied [1-3]. These studies reveal that for monolayer hexane, there are three distinct phases observed. The first is the solid HB phase that exists at low temperatures and is commensurate with the graphite substrate. With increasing temperature, and by $T=150K$, they [2-3] observe a transition into a rectangular phase that seems to coexist with a liquid. This phase persists until $T=176K$ where all order is lost in the system and melting into an isotropic fluid ensues.

Similarly for submonolayer hexane, experiment [1-3] suggests the molecules arrange in a uniaxially incommensurate (UI) structure on the substrate at low temperatures, evolving continuously into a fully commensurate structure at completion. Further study [3] of this structure gives indication of low-density light domain walls existing below coverages of $\rho=0.92$ that seem to be filled by a fluid. These domain walls are observed to be commensurate, except near the domain walls, where the molecules relax from commensurate positions, and melting is observed to occur from such structures.

Previous simulations [4-8] have been carried out studying monolayer hexane on graphite, which confirm the presence of the three phases and present an elegant theory by which melting in such systems takes place by means of a "footprint reduction," [4] rather than exhibiting properties of the KTHNY theory of melting in 2D. These simulations initially observe that conformation changes are responsible for the melting transition in hexane. However, more recent simulations [5-7] show that through the use of parameters more accurately representing the surface interaction [5], the melting transition occurs at a lower temperature with a large presence of molecules tilted out of the surface plane. There has been no known theoretical work completed regarding the anomalous behavior of submonolayer or supermonolayer hexane on graphite.

2 MODEL AND METHODS

The model that is used in all simulations has been described in detail elsewhere [8] and so will only be briefly described here. In all cases, we use a molecular dynamics method to simulate 112 hexane molecules at coverages of $\rho=0.87$ to $\rho=1.05$ on the graphite surface. The UA model [9] is used in most cases, which combines each methyl and methylene group into a single psuedoatom, with the two different groups distinguished only by mass and a different Van Der Waals radius. For submonolayer hexane, the anisotropic united-atom (AUA4) model [10] is also used which is anisotropic in that it treats the tetrahedral symmetry in the methyl groups and extends the psuedoatom position closer to the hydrogen atoms in the methylene groups. To modify the coverage, the computational cell is expanded along the *b*-direction of the oblique unit cell to
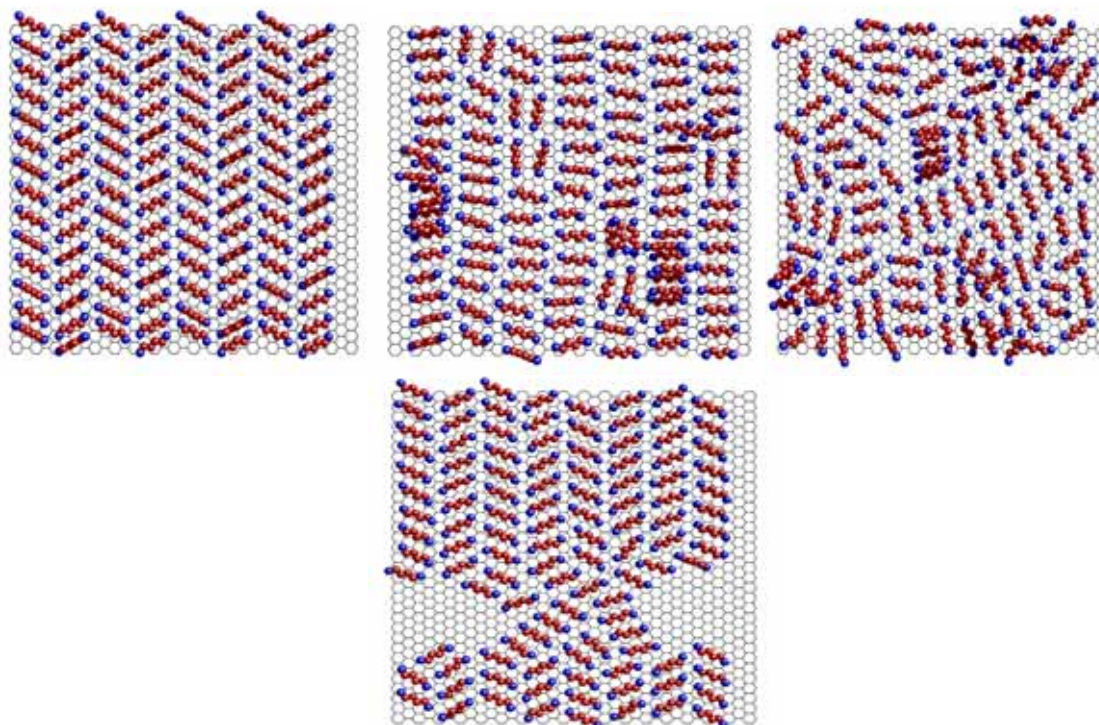
Figure 1. (Top) Snapshots of the three phases observed in hexane on graphite. These are the low temperature herringbone phase (left), the intermediate nematic phase (middle), and the isotropic fluid phase (right). Also, (bottom) the low temperature phase for ρ=0.875 is shown that is comprised of commensurate herringbone solid structures with ρ=1 on either side of a low-density fluid filled domain wall.

preserve the commensurability in the *a*-direction (which is most important). Periodic boundary conditions are used in the plane parallel to the substrate, and each simulation is begun from a low-temperature HB phase consistent with experimental observations [3]. To maintain temperature stability, the velocities are rescaled to satisfy equipartition for the center-of-mass, translational, and rotational velocities. A velocity Verlet RATTLE [11] algorithm is used to integrate the equations of motion as well as to constrain the fast C-C stretching modes to their equilibrium value. All simulations are carried out for a total of 700 ps with a period of 500 ps over which averages are taken.

The intermolecular interactions are modeled by a 12-6 Lennard Jones pair potential with Lorentz-Berthelot rules describing mixed interactions. The surface interaction is modeled by a Fourier expansion proposed by W.A. Steele [12] that assumes an isotropic surface of infinite extent in the *xy* plane, and semi-infinite in the –*z* direction. Since the bond-lengths are constrained, the intramolecular potential is composed of two terms representing the C-C-C bond angle bending [9] and the torsion of the molecules [6,13]. Again, details regarding these interactions and the para-meters involved in their potentials are given elsewhere [8].

3 RESULTS AND DISCUSSION

A series of snapshots are presented in figure 1 that represent (top) the three phases that are observed in the study of hexane on graphite and (bottom) the domain walls observed when the AUA4 model is used at the submonolayer coverage of ρ=0.875. These give a good representation of the structure of the system in each observed phase. The behavior of submonolayer hexane with the UA model is similar to that of monolayer hexane at low temperatures with the exception that HB phase is "stretched" in the *y*-direction (uniaxially incommensurate).

In figure 2, the bond-roll angle, $P(\Psi)$, distribution is presented where Ψ is defined as:

$$\psi = \cos^{-1}\left[\frac{\left\{(\vec{r}_{j+1}-\vec{r}_j)\times(\vec{r}_{j-1}-\vec{r}_j)\right\}\cdot\hat{z}}{\left|(\vec{r}_{j+1}-\vec{r}_j)\times(\vec{r}_{j-1}-\vec{r}_j)\right|}\right]. \qquad (1)$$

In equation 1, the values of $\vec{r}$ represent the psuedoatom positions of three consecutive psuedoatoms in a molecule. The cross product therefore involves two vectors that extend from an innermost psuedoatom to two bonded neighbors. The dot product in the numerator is zero when the backbone of the molecule is rigid with the surface (when the molecule is rolled normal to the substrate), and Ψ=90°. If the reverse is true, where the molecule lies flat in the surface plane, the quantity inside the brackets in
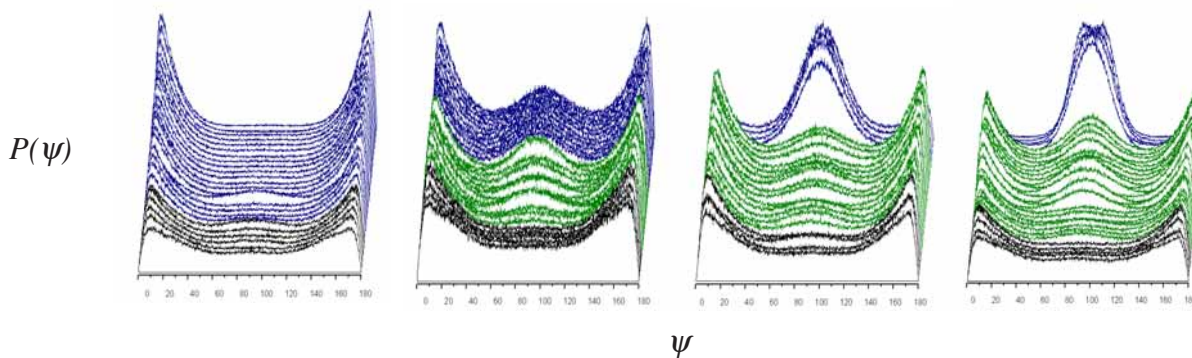
Figure 2. Bond roll angle distributions $P(\Psi)$ for submonolayer (two on left), and supermonolayer (two on right) densities. The value of Ψ is 90° when the molecule is perpendicular to the plane of the substrate, and is 0° and 180° when the molecule is parallel to the plane of the substrate. The blue lines correspond to temperature points in the herringbone, the green lines correspond to points in the nematic, and the black lines correspond to the isotropic fluid. The second plot corresponds to the submonolayer density exhibiting the weak nematic phase. The average density increases from left to right.

equation (1) assumes a value of 1, which gives Ψ=0° or 180°. Therefore, a large peak at Ψ=90° in figure 2 for supermonolayer coverages indicates that the majority of the molecules are rolled normal to the substrate, whereas for submonolayer coverages, $P(\Psi)$ indicates that there is very little to no in-plane rolling of the molecules. Although the presence of the intermediate phase is clearly augmented from an increasing coverage by inspection of figure 2, table 1 gives a quantitative representation of the simulated transition temperatures that are observed for each coverage studied with the UA model. These transition temperatures are composed through study of averaged order parameters, energies, and correlation functions that are monitored through each simulation. The results seem to suggest that the intermediate phase is dramatically affected by the increase/decrease of coverage, however, the melting transition temperature stays fairly consistent until the lowest coverage, which we find is where the UA model breaks down and fails to represent this system in terms of both structure and transition temperatures.

3.1 Observed Phases

In most cases, the three phases that we observe are those that have been both observed experimentally as well as in previous theoretical work. The intermediate phase, however, we find exhibits order that is similar to a liquid crystal, and although systems of 112 molecules are not large enough to fully indicate that there is fluid coexisting with a solid, simulations of 336+ hexane molecules shows that between T=160-175K, there is a significant amount of disordered molecules that exist around a cell of orientationally ordered molecules. This indicates that the nematic phase shown in figure 1 is representative of the solid-liquid coexistance region that has been observed experimentally [1-3] to exist between the solid and liquid

ρ	T_1 (K)	T_2 (K)
0.875	N/O	155±3
0.9	N/O	172±3
0.93	N/O	174±3
0.965	155±5	175±3
1.0	138±2	176±3
1.02	122±3	172±3
1.035	98±3	175±3
1.05	85±3	175±3

Table 1. Intermediate and melting transition temperatures, T_1 and T_2, for each coverage studied. The use of "N/O" refers to a transition that is not observed. All temperatures are in units of Kelvin and all uncertainties are noted.

phase. The observation that this coexistance region continuously loses solid properties until the melting transition is in agreement with the fact that we only observe coexistance over the latter portion of the nematic phase.

There are some distinct differences that are present structurally in the intermediate phase as the coverage is increased. First of all, we find the intermediate phase is preempted by layer promotion that is a result of molecular interactions that cause molecules to tilt out of the surface plane and promote to the bilayer. This action causes vacancies in the monolayer and if the molecules are not tightly packed (i.e. coverages greater then completion), then in some cases, the molecules will be free to orient normal to the director angle. This is evident in figure 1 where five groups of 2 hexanes orient normal to the monolayer system orientation. However, for higher coverages, the molecules *all* tend to a single orientation because there is less in-plane space for them to undergo such an orientational change.

This gives rise to an increased value for the nematic order parameter as well (not shown).

The other phase that is of interest is the low-temperature HB phase. For submonolayer hexane, through use of the UA model, the HB phase is uniaxially incommensurate under all circumstances until the model breaks down at a coverage of ρ=0.875. Experiment suggests that a UI HB structure is observed for coverages greater than ρ=0.92, but below this coverage, the formation of light domain walls with a proposed fluid occupying the domain wall is observed. Simulations that use the AUA4 model for ρ=0.875 show that the low-temperature HB phase involves the presence of domain walls with domain wall spacing of about 8-12a_g, which seems to be consistent with experiment for the most part. Also, the molecular relaxation near the domain wall is also observed, as shown in figure 1. However, the melting temperature of the system is very low with AUA4 model, but this could arise from a number of effects including finite size effects and periodic boundary conditions as well as the initial UI configurations that all simulations are started from.

3.2 Observed Transitions

The transition temperatures observed are presented in table 1 with their respective uncertainties. The melting transition in all cases seems to be consistent at about T=175K for all coverages that are studied. However, the intermediate transition temperatures are far more dependent upon coverage than the melting temperatures.

Previous work on this system has found that it obeys the space reduction theory previously proposed [4-7], but it has been unclear how this space reduction takes place. We find that the dihedral distribution (not shown) gives indication that there are gauche molecules present near the melting transition, but this gives no quantitative explanation for how these affect the transition. To elucidate this melting behavior, we simulate the monolayer with constants in the torsional potential increased by 10x (to constrain the molecules from undergoing conformation changes). We find that the melting transition is increased by ca. 20K, which indicates that gauche defects do contribute to the melting transition, but the contribution is not very significant due to the effects of out-of-plane tilting. This shows the footprint reduction in this system is cooperative between these two space reduction mechanisms with out-of-plane tilting playing the lead role.

For the intermediate phase, we find that the footprint reduction is *also* satisfied through layer promotion. The promotion of molecules to the 2nd layer creates a number of in-plane vacancies that preempt a phase transition into the intermediate phase. We notice that the intermediate phase transition occurs at lower temperatures when the in-plane space is reduced, which means that the molecules are undergoing more intermolecular "collisions", which provide them with more kinetic energy to tilt out of the surface plane at lower temperatures and for some molecules

to simultaneously promote to the 2nd layer. We also find a relationship between the in-plane rolling of the molecules normal to the substrate and the in-plane space available (figure 2). With less in-plane space, the molecules assume a less energetically favorable position (rolled normal to the substrate) which indicates that the intermolecular kinetic energy is higher in the system, however, upon the transition into the nematic-ordered phase, the molecules relax and roll back on their sides until the melting transition. This is also evident from inspection of the average Lennard-Jones interaction energy (not shown), which indicates that the interaction energy is minimized at this intermediate transition.

Therefore, we find that the transitions in this study and the intermediate phase are a result of the effects that come about due to space reduction in the system. We conclude that understanding the effects of in-plane space in this and similar systems is a fundamental part of understanding the behavior of the transitions and the phases.

REFERENCES

[1] T. Arnold, R.K. Thomas, M.A. Castro, S.M. Clarke, L. Messe, and A. Inaba, Phys. Chem. Chem. Phys. 4, 345-51, 2002.

[2] J. Krim, J. Suzanne, H. Shechter, R. Wang, and H. Taub, Surf. Sci. 162, 446, 1985.

[3] J.C. Newton, Ph.D. dissertation, University of Missouri-Columbia, unpublished, 1989.

[4] F.Y. Hansen and H. Taub, Phys. Rev. Lett. 69, 652, 1992.

[5] E. Velasco and G.H. Peters, J. Chem. Phys. 102, 1098, 1995.

[6] G.H. Peters and D.J. Tildesley, Langmuir 12, 1557 1996.

[7] G.H. Peters, Surf. Sci. 347, 169, 1996.

[8] M.W. Roth, C.L. Pint, C. Wexler, Phys. Rev. B (in press)

[9] M.G. Martin and J.I. Siepmann, J. Phys. Chem. 102, 2569, 1998.

[10] P. Ungerer, C. Beauvais, J. Delhommelle, A. Boutin, B. Rousseau, and A.H. Fuchs, J. Chem. Phys. 112, 5499, 2000.

[11] M. P. Allen and D.J. Tildesley, "Computer Simulation of Liquids," Clarendon Press, New York, 1988.

[12] W.A. Steele, Surf. Sci. 36, 317, 1973.

[13] P. Padilla and S. Toxvaerd, J. Chem. Phys. 94, 5650, 1991.